PROCESS MODEL FOR AMMONIA VOLATILIZATION FROM ANAEROBIC SWINE LAGOONS INCORPORATING VARYING WIND SPEEDS AND GAS BUBBLING

K. S. Ro, A. A. Szogi, M. B. Vanotti, K. C. Stone

ABSTRACT. *Ammonia volatilization from treatment lagoons varies widely with the total ammonia concentration, pH, temperature, suspended solids, atmospheric ammonia concentration above the water surface, and wind speed. Ammonia emissions were estimated with a process-based mechanistic model integrating ammonia chemistry of the lagoon and interfacial transport characteristics between air and water. This improved model incorporated the effect of internal bubble production and continuously variable wind speed on ammonia volatilization measured at 10 m above the liquid surface (U_{10}). Model simulations were compared to ammonia emission rates measured simultaneously at three contrasting lagoon scenarios: non-treated lagoon (13,633 kg ha^{-1} year^{-1}), partially pre-treated manure using solid-liquid separation (3,699 kg ha^{-1} year^{-1}), and treated manure using combined solid-liquid separation with nitrogen and phosphorus removal from the liquid (1,311 kg ha^{-1} year^{-1}). The simulations only using average U_{10} with bubble enhancement or U_{10} distributions without bubble enhancement produced fluxes 42% and 44% below observed fluxes, respectively. However, the simulated fluxes using the U_{10} distributions along with bubble enhancement for the non-treated lagoon during warm seasons closely matched the observed fluxes ($y = 1.04x$, with $R^2 = 0.76$). Ammonia emissions would be significantly underpredicted if bubbling-enhanced mass transport was not taken into account during warm seasons, as demonstrated by the improved process model and evidenced by the observed fluxes.*

Keywords. *Ammonia volatilization, Anaerobic treatment lagoon, Bubbles, Process model, Wind speed.*

Anaerobic treatment lagoons have been widely utilized for storage before land application and as partial treatment technology for wastewater from concentrated animal feeding operations (CAFOs) in the Southeast and Midwest. Flushed manure from animal houses is discharged into these lagoons in which various physico-chemical and biological treatment processes take place and substantially reduce suspended solids, chemical oxygen demand (COD), and nitrogenous compounds such as ammonia. A significant portion of ammonia in the treatment lagoons is volatilized into the atmosphere because of very low dissolved oxygen available for biological nitrification to take place. Ammonia emission from these treatment lagoons of CAFOs is a major concern because ammonia is a principle source of atmospheric aerosols and contributes to the regional acidification problems (Arogo et al., 2003a; Bajwa et al., 2006; Blunden and Aneja, 2007; USEPA, 2001).

The volatilization of ammonia from treatment lagoons varies widely with the total ammonia concentration, temperature, suspended solids, pH of lagoon liquid, atmospheric ammonia concentration above the water surface, and wind speed (Arogo et al., 1999; Arogo et al., 2003a; De Visscher et al., 2002; Harper et al., 2004; Liang et al, 2002; Ni, 1999). The total ammonia concentration, pH, ionic strength, temperature, and suspended solids of lagoon liquid determine the degree of dissociation of ammonia, i.e., volatile free ammonia (NH_3) and non-volatile ammonium ion (NH_4^+). Wind produces turbulence in lagoon liquid and convective transport of atmospheric ammonia above the water surface, facilitating the ammonia volatilization process. As a result, ammonia volatilization increases with wind speed (Arogo et al., 1999; Arogo et al., 2003b; De Visscher et al., 2002; Harper et al., 2000; Harper et al., 2004; Liang et al., 2002; Monteny, 2000; Ni, 1999).

Wind-driven ammonia volatilization rates from treatment lagoons are difficult to measure and require specialized techniques and equipment. Not only did reported values of ammonia volatilization rate vary widely with different lagoons and seasons (i.e., from 0.3 to 199 kg NH_3–N ha^{-1} d^{-1}), but different measurement methods used on overlapping days for the same lagoon also produced widely different volatilization rates. For instance, the ammonia volatilization rates measured by a micrometeorological method from a primary anaerobic swine lagoon were 15.4 to 22 kg NH_3–N ha^{-1} d^{-1} during 6-9 August 1997, which contrasted with the ammonia volatilization rates measured by the chamber method of 34 to

Submitted for review in June 2007 as manuscript number SE 7051; approved for publication by the Structures & Environment Division of ASABE in November 2007.

Mention of a trade name, proprietary product, or vendor does not constitute a guarantee or warranty of the product by the USDA and does not imply its approval to the exclusion of other products or vendors that also may be suitable.

The authors are **Kyoung S. Ro, ASABE Member Engineer,** Environmental Engineer, **Ariel A. Szogi, ASABE Member,** Soil Scientist, **Matias B. Vanotti, ASABE Member Engineer,** Soil Scientist, and **Kenneth C. Stone, ASABE Member Engineer,** Agricultural Engineer, USDA-ARS Coastal Plains Soil, Water, and Plant Research Center, Florence, South Carolina. **Corresponding author:** Kyoung S. Ro, USDA-ARS, 2611 West Lucas St., Florence, SC 29501; phone: 843-669-5203, ext. 107; fax: 843-669-6970; e-mail: Kyoung.Ro@ars.usda.gov.

  ISSN 0001–2351

123 kg NH_3-N ha^{-1} d^{-1} from the same lagoon during 1-15 August 1997 (table 5 of Arogo et al., 2003a). It is not clear what caused this much difference in ammonia volatilization rates, except that each method has its own inherent weaknesses and that measurements taken for a few hours to a few days represent at best snapshot views of continuously varying ammonia volatilization rates from the lagoon.

Ammonia volatilization rates from anaerobic swine lagoons can also be estimated with process-based mechanistic models incorporating the ammonia chemistry of the lagoon and interfacial transport characteristics between air and water (Arogo et al., 1999; Arogo et al., 2003b; Bajwa et al., 2006; De Visscher et al., 2002; Liang et al., 2002). These process models enable us to estimate ammonia volatilization rates based on easily measurable water quality and micrometeorological parameters such as temperature, pH, ammonia concentration, and wind speed. Most of these models utilize ammonia and other gas mass transfer coefficients determined from wind tunnel studies with well-defined wind conditions. However, unlike the wind tunnel studies, wind speed varies almost continuously in the field. Arithmetic mean wind speeds have frequently been used as characteristic wind speeds. Unless the ammonia volatilization is linearly dependent upon wind speed, a simple arithmetic average wind speed will not adequately characterize the ammonia volatilization process in the field. Several studies have reported that gas transfer depends nonlinearly on wind speed (Macintyre et al., 1995; Ro and Hunt, 2006; Upstill-Goddard et al., 1990; Wanninkhof, 1992).

Biogas frequently observed in anaerobic treatment lagoons during warm seasons further complicates ammonia volatilization process models (Hamilton et al., 2006; Harper et al., 2000; Safley and Westerman, 1988; Sharpe and Harper, 1999). As the bubbles rise through the water column, turbulence is created because of the drag force created at the water-bubble interface. This additional turbulence enhances the ammonia volatilization process in anaerobic treatment lagoons. Furthermore, ammonia can be volatilized into the bubbles and directly conveyed to the atmosphere with the bubbles. To date, no process-based ammonia volatilization model has accounted for the effects of biogas production on ammonia volatilization from anaerobic treatment lagoons.

The objectives of this study were to: (1) develop an ammonia volatilization process-based model incorporating the effects of internal bubbling, and (2) introduce a new methodology in characterizing continuously varying wind speed for ammonia volatilization using the Weibull probability density function. By implementing these new concepts, we believe that a more accurate process model for prediction of ammonia emission from treatment lagoons can be developed.

Model Development

Air-water interfacial ammonia transport characteristics have been largely modeled based on the two-film theory (Lewis and Whitman, 1924). The theory assumes that the entire resistance to interfacial mass transfer occurs in thin laminar films of each phase. In other words, it assumes that there is no mass transfer resistance in the bulk fluid. The ammonia flux from the lagoon surface based on the two-film theory is expressed as:

$$J_N = k_L\left(C_{N,B} - C_{N,i}\right) = k_G\left(P_{N,i} - P_{N,B}\right) \quad (1)$$

where

J_N = ammonia flux from lagoon (kg m^{-2} s^{-1})
k_L = individual liquid-phase mass transfer coefficient (m s^{-1})
k_G = individual gas-phase mass transfer coefficient (m s^{-1})
$P_{N,i}$ = air-phase ammonia nitrogen concentration in the interface (kg m^{-3})
$P_{N,B}$ = ammonia nitrogen concentration in the bulk air (kg m^{-3})
$C_{N,B}$ = free ammonia concentration in the bulk liquid (kg m^{-3})
$C_{N,i}$ = free ammonia concentration in the interface (kg m^{-3}).

Assuming an instantaneous equilibrium at the interface that can be adequately described by Henry's law (Cussler, 1984; Gottschalk et al., 2000), the interfacial concentrations in equation 1 can be eliminated as:

$$J_N = K_L\left(C_{N,B} - \frac{P_{N,B}}{K_H}\right) = K_L\left(FC_{T,B} - \frac{P_{N,B}}{K_H}\right) \quad (2)$$

where

$C_{T,B}$ = total ammonia species concentration in the bulk liquid phase (kg m^{-3})
$C_{T,i}$ = total ammonia species concentration in the liquid interface (kg m^{-3})
K_H = Henry's constant for ammonia (dimensionless), $K_H = \frac{P_{N,i}}{C_{N,i}} = \frac{P_{N,i}}{F \cdot C_{T,i}}$
F = fraction of free ammonia (dimensionless)
K_L = overall liquid-phase mass transfer coefficient (m s^{-1}), $K_L = \frac{k_L k_G K_H}{k_G K_H + k_L}$.

The two-film theory allows the additivity of the interfacial mass transfer resistances as the sum of gas-film resistance and liquid-film resistance. This additivity of resistance can be visualized by rearranging the overall liquid-phase mass transfer coefficient as:

$$R_T = \frac{1}{K_L} = \frac{1}{k_L} + \frac{1}{k_g K_H} = R_L + R_g \quad (3)$$

where

R_T = total resistance (s m^{-1})
R_L = liquid-phase resistance (= $1/k_L$, s m^{-1})
R_G = gas-phase resistance (= $1/k_G K_H$, s m^{-1}).

The success of using equation 2 for estimating ammonia volatilization rates from lagoons critically depends upon accurate estimating of the equilibrium and transport parameters (i.e., F, K_H, k_L, and k_G).

Fraction of Free Ammonia in Lagoon Liquid

The degree of ammonia dissociation in the lagoon liquid is much lower than that of clean water (deionized water). One-half to one-sixth of theoretical values of the dissociation constant for treatment lagoon liquid were reported in the literature (Arogo et al., 2003b; De Visscher et al., 2002; Liang et al., 2002; Zhang, 1992). The lower values of the dissociation constant were attributed to the large deviation of activi–

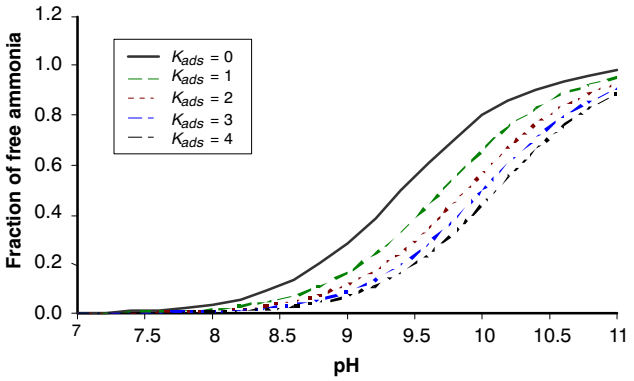

Figure 1. Fraction of free ammonia at different values of K_{ads} at 20°C.

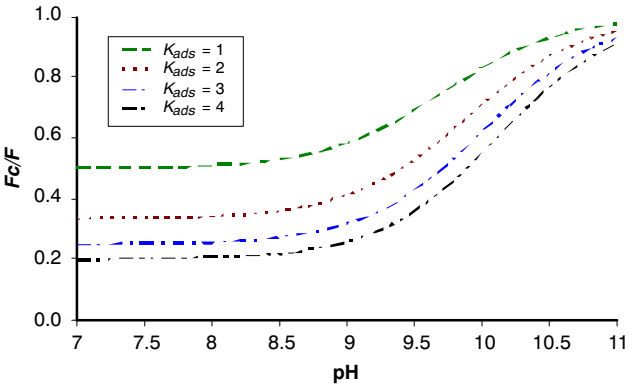

Figure 2. Ratio of F_C/F at various pH (fig. 1).

ty coefficients of ammonia species and hydrogen ions from unity because of higher ionic strength of lagoon liquid and adsorption of NH_4^+ on the suspended solids (De Visscher et al., 2002; Arogo et al., 2003b). De Visscher et al. (2002) introduced a lumped parameter called the equilibrium constant of the adsorption of ammonia on the suspended organic material and expressed the fraction of free ammonia in lagoon liquid as:

$$F_C = \frac{1}{1+10^{-pH}\left(1+K_{ads}\right)/K_{a,w}} \quad (4)$$

where

F_C = corrected fraction of free ammonia in lagoon liquid
$K_{a,w}$ = dissociation constant for NH_4^+ in clean water
K_{ads} = equilibrium constant for ammonia adsorption.

Although K_{ads} was named as the equilibrium constant for ammonia adsorption on suspended solids, it is really a lumped parameter accounting for all other phenomena contributing to the deviation of the dissociation constant from that of clean water. The deviation could also be partly caused by the departure of activity coefficients of ions from unity because of high ionic strength of lagoon liquid.

De Visscher et al. (2002) reported that K_{ads} of 3.0 generally yielded good agreement between the measured and modeled fluxes. As shown in figure 1, higher values of K_{ads} reduce the fraction of free ammonia at a given pH. At a typical lagoon liquid pH of 7.8, K_{ads} of 3.0 reduces the fraction of free ammonia 25% less than that of clean water (fig. 2). The difference between F_C and F diminishes at higher pH. Interestingly, Arogo et al. (2003b) reported that apparent dissociation constants (K_a) for swine lagoon liquid at 35°C, 25°C, and 15°C were 50%, 51%, and 94%, respectively, of that for clean water. These K_a values for lagoon liquid correspond to K_{ads} = 1 in equation 4 except at 15°C. Because Arogo et al. (2003b) measured the values of dissociation constants more directly than from fitting the flux model, as done by De Visscher et al. (2002), we used K_{ads} = 1 for our new mathematical flux model simulations.

Henry's Law Constants

Liang et al. (2002) evaluated various Henry's law constant equations for ammonia. They concluded that the equation developed by Anderson et al. (1987) was the most relevant for swine lagoons. Similarly, we also used the non-dimensional form of Henry's law constant for ammonia, as reported by Liang et al. (2002):

$$K_H = \frac{2.395\times10^5}{T+273.16}\exp\left(\frac{-4151}{T+273.16}\right) \quad (5)$$

where T = temperature (°C).

Mass Transfer Coefficients

The gas- and liquid-phase mass transfer coefficients for ammonia in equations 2 and 3 are usually estimated from that for H_2O and O_2, respectively. Because there is no liquid-phase mass transfer resistance for water vapor in water, the overall mass transfer coefficient for water vapor is equal to the gas-phase mass transfer coefficient according to equation 3. For oxygen, gas-phase mass transfer resistance is negligible; as a result, the overall mass transfer coefficient for O_2 is usually assumed to be the liquid-phase mass transfer coefficient (Hsieh et al, 1993). The mass transfer coefficients for ammonia are then estimated by:

$$\frac{k_1}{k_2} = \left(\frac{D_1}{D_2}\right)^n \quad (6)$$

where

k_1 or k_2 = mass transfer coefficient of species 1 or 2 (m s^{-1})
D_1 or D_2 = diffusivity of species 1 or 2 (m^2 s^{-1})
n = power index, usually 0.67 for gas-phase and 0.5 for liquid-phase coefficients.

The gas-phase mass transfer coefficient for water vapor was estimated using the correlation developed by Mackay and Yeun (1983). Water vapor mass transfer coefficients at different wind speeds were estimated based on the amount of water evaporated. The correlation was normalized to 10 m wind speed. This equation also adequately predicted the water vapor mass transfer coefficients observed by Liss (1973):

$$k_{G,w} = 46.2\times10^{-5}\left(6.1+0.63U_{10}\right)^{0.5}U_{10}Sc_{G,w}^{-0.67}$$

$$\text{for } U_{10} > 0 \quad (7)$$

where

$k_{G,w}$ = water vapor gas-phase mass transfer coefficient (m s^{-1})
U_{10} = wind speed at 10 m above water surface (m s^{-1})
$Sc_{G,w}$ = Schmidt number for water vapor = $\frac{\mu_a}{\rho_a D_{a,w}}$
μ_a = dynamic viscosity of air (N s m^{-2})

ρ_α = air density (kg m^{-3})
$D_{a,w}$ = diffusivity of water vapor in the air (m^2 s^{-1}).

The gas-phase mass transfer coefficient for ammonia is then estimated using equations 6 and 7. The ammonia liquid-phase mass transfer coefficient was estimated using the new surficial oxygen transfer coefficient correlation derived from the published data for the last 50 years (Ro and Hunt, 2006):

$$k_{L,O2} = \left[170.6 \cdot Sc_{L,O2}^{-1.2} U_{10}^{1.81} \left(\frac{\rho_a}{\rho_w} \right)^{1/2} \right] \cdot 2.78 \times 10^{-6} \quad \text{for } U_{10} > 0 \tag{8}$$

where

$k_{L,O2}$ = oxygen liquid-phase mass transfer coefficient (m s^{-1})

$Sc_{L,O2}$ = Schmidt number for oxygen in water = $\dfrac{\mu_w}{\rho_w D_{w,02}}$

μ_w = dynamic viscosity of water (N s m^{-2})
ρ_ω = water density (kg m^{-3})
$D_{w,O2}$ = diffusivity of oxygen in water (m^2 s^{-1}).

Densities and viscosities of air and water were calculated based on third-order polynomial interpolations of published data (Crowe et al., 2001). Diffusivities of ammonia, oxygen, and water vapor were estimated from existing correlations (Frank et al., 1996; Fuller et al., 1966; Wanninkhof, 1992). These equations are summarized in table 1.

Enhanced Ammonia Volatilization by Biogas Formation in Anaerobic Treatment Lagoons

Production of biogas (mainly CH_4 and CO_2) has been observed in treatment lagoons for animal wastes (Safley and Westerman, 1988; Hamilton et al., 2006). Interestingly, significant amounts of dinitrogen gas were observed in swine waste lagoons where the classical nitirificaton-denitrification pathway was not expected because of lack of nitrates in the lagoons, a precursor for denitrification (Harper et al., 2000). These biogas bubbles rise in the treatment lagoon liquid column caused by density difference. The rise of bubbles creates turbulence caused by drag force exerted at the bubble surface. The turbulence in the water enhances the ammonia mass transfer, especially in the interfacial regions. In addition to the increase in turbulence, ammonia can also be transported directly into bubbles and conveyed to the air above the water surface with the bubbles, as illustrated in figure 3. The increase in turbulence in the water column and the conveying of ammonia via bubbles enhances the ammonia volatilization process. This bubble-enhanced ammonia volatilization process in treatment lagoons has not been studied to date, nor does this article attempt to mechanistically model this complicated process. Instead, we propose to modify the resistance-in-series concept (i.e., eq. 3) and introduce the enhanced mass transfer of ammonia by biogas bubbles as a reduction to the overall resistance:

$$R_T = \frac{1}{K_{L,B}} = \frac{1}{k_{L,B}} + \frac{1}{k_G K_H} = \frac{1}{k_L} + \frac{1}{k_G K_H} - R_B$$

$$= R_L + R_G - R_B \quad \text{for } |R_B| \le R_L + R_G \tag{16}$$

Table 1. Properties of air, water, ammonia, and oxygen.

Density:

$\rho_a = 1.29 - 4.80 \times 10^{-3} T + 3.00 \times 10^{-5} T^2 - 9.00 \times 10^{-8} T^3$ (9)

$\rho_w = 999.84 + 6.79 \times 10^{-2} T - 9.10 \times 10^{-3} T^2 + 1.00 \times 10^{-4} T^3$ (10)

where

ρ_a = air density (kg m^{-3})
ρ_w = water density (kg m^{-3})
T = temperature (°C).

Viscosity:

$\mu_a = 2.00 \times 10^{-5} + 5.00 \times 10^{-8} T - 2.00 \times 10^{-10} T^2 + 1.00 \times 10^{-11} T^3$ (11)

$\mu_w = 1.80 \times 10^{-3} - 6.00 \times 10^{-5} T + 1.00 \times 10^{-6} T^2 - 1.00 \times 10^{-8} T^3$ (12)

where

μ_a = air viscosity (N s m^{-2})
μ_w = water viscosity (N s m^{-2}).

Diffusivity in air:

$$D_{a,i} = \frac{1.00 \cdot 10^{-7} (273.15 + T)^{1.75} (1/M_a + 1/M_i)^{0.5}}{P \left[(\sum_a \upsilon_a)^{1/3} + (\sum_i \upsilon_i)^{1/3} \right]^2} \tag{13}$$

where

$D_{a,i}$ = diffusivity of i in the air (m^2 s^{-1})
M_a = molecular weight of air (28.9 g mol^{-1})
M_i = molecular weight of i
$(\Sigma v)_a$ = diffusion volume of air (20.1 cm^3 mol^{-1})
$(\Sigma v)_i$ = diffusion volume of i (14.9 and 12.7 cm^3 mol^{-1} for NH_3 and H_2O, respectively)
P = pressure (atm).

Diffusivity in water:

$D_{w,N} = (1.65 + 2.47 x_N) \times 10^{-6} \exp\{-16600/[R(273.15 + T)]\}$ (14)

$D_{w,O2} = (\mu_w/\rho_w)(1800.60 - 120.10T + 3.78T^2 - 4.76 \times 10^{-2} T^3)$ (15)

where

$D_{w,N}$ = diffusivity of NH_3 in water (m^2 s^{-1})
$D_{w,O2}$ = diffusivity of O_2 in water (m^2 s^{-1})
x_N = mole fraction of NH_3 in water
R = universal gas constant (8.314 J K^{-1} mol^{-1}).

where

$K_{L,B}$, $k_{L,B}$ = bubble-enhanced mass transfer coefficients (m s^{-1})
R_B = mass transfer resistance due to bubble presence (s m^{-1}).

The bubbling affects only liquid-phase mass transport, as shown in equation 16. It is important to notice that under extreme conditions of very large liquid-phase mass transfer coefficient, the total resistance may become negative, and

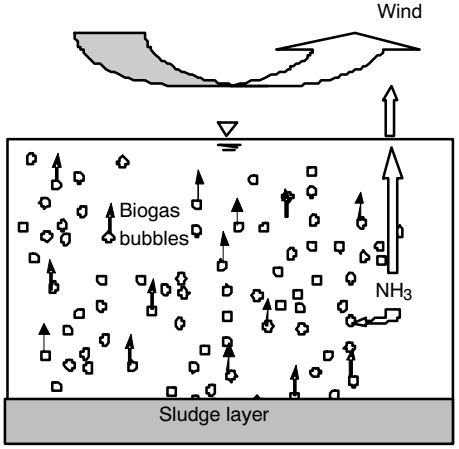

Figure 3. Bubble-enhanced ammonia volatilization in treatment lagoons.

equation 16 should not be used in that case. The bubble-enhanced mass transfer coefficients can be estimated from the correlation developed by Hsieh (1991), who reported that volatile organic compounds and oxygen mass transfer rates increased with specific airflow rates in bubble aeration columns. Hsieh (1991) reported that oxygen liquid-phase mass transfer coefficients under aeration could be estimated with specific airflow rates as:

$$k_{L,O2} = \frac{1}{3600}\left[1.35\left(\frac{Q}{V}\right)^{0.37}\right] \quad (17)$$

where

$k_{L,O2}$ = liquid-phase oxygen mass transfer coefficient (m s^{-1})
Q = airflow rate (L h^{-1})
V = reactor volume (L).

Equations 6 and 17 can be used to estimate the bubble-enhanced mass transfer coefficient for ammonia in treatment lagoons. However, applicability of equation 17 for treatment lagoons still needs to be carefully evaluated because the specific biogas production range (0.001 to 0.01 h^{-1}) reported by Safley and Westerman (1988) is much lower than the specific aeration rate range (1.6 to 7.2 h^{-1}) used in establishing equation 17.

Mean Mass Transfer Coefficient for a Field Site with Varying Wind Speed

Empirical and semi-empirical correlations exist in the literature for wind-driven air-water interfacial mass transfer coefficients, as recently reviewed by Ro et al. (2007). Most of these correlations show that values of mass transfer coefficients are strongly dependent on wind speed. However, the wind speed above a lagoon varies almost continuously in the field. Arithmetic mean wind speeds have frequently been used as characteristic wind speeds; yet gas transfer depends nonlinearly upon wind speed (Macintyre et al., 1995; Ro and Hunt, 2006; Upstill-Goddard et al., 1990; Wanninkhof, 1992). Unless the mass transfer coefficients are linearly dependent upon wind speed, a simple arithmetic average wind speed will not adequately characterize the nonlinearity of a wind-driven ammonia volatilization process in the field. A potential solution is to integrate the product of a characteristic wind speed distribution for a field site and the instantaneous transfer coefficient over the entire range of wind speed:

$$\overline{K}_L = \int_0^\infty f(U_{10}) \cdot K_L(U_{10}) \cdot dU_{10} \quad (18)$$

where

$f(U_{10})$ = wind speed distribution function
$\overline{K}_L$ = mean overall liquid-phase mass transfer coefficient (m s^{-1})
$K_L(U_{10})$ = overall liquid-phase mass transfer coefficient as a function of U_{10} (m s^{-1}).

Ro and Hunt (2007) successfully used the Weibull probability density function to characterize the wind speed variations in Florence, South Carolina. The two-parameter Weibull probability distribution function is given by:

$$f(U_{10}) = \frac{\beta}{\lambda}\left(\frac{U_{10}}{\lambda}\right)^{\beta-1} \exp\left[-\left(\frac{U_{10}}{\lambda}\right)^{\beta}\right] \quad \text{for } U_{10} > 0 \quad (19)$$

Otherwise, $f(U_{10}) = 0$

where β is a shape parameter and λ is a scaling factor.

Troen and Peterson (1989) showed that in northern Europe the values of β were close to 2 for the fitted Weibull distributions of wind speeds. Ro and Hunt (2007) reported that β = 1.9 and λ = 2.8 effectively characterized the 2005 wind speed distribution in Florence, South Carolina. Combining equations 18 and 19, the mean overall liquid-phase transfer coefficient can be estimated by:

$$\overline{K}_L = \int_0^\infty K_L(U_{10}) \frac{\beta}{\lambda}\left(\frac{U_{10}}{\lambda}\right)^{\beta-1} \exp\left[-\left(\frac{U_{10}}{\lambda}\right)^{\beta}\right] \cdot dU_{10} \quad (20)$$

Methodology

Bubble-Enhanced Ammonia Volatilization

The experimental site was on a grass plain of the USDA-ARS Coastal Plains Soil, Water, and Plant Research Center in Florence, South Carolina. Two galvanized-iron evaporation pans (1.2 m diameter × 0.24 m depth) and two clear PVC columns (0.15 m diameter × 0.69 m depth) were embedded into the ground in such a way that the top of the container was parallel to the ground surface. One of the pans or columns was aerated with a compressed air cylinder, a Cole Palmer 150 mm flow tube meter with a needle value, and a small diffusion stone (4.0×10^{-5} to 9.2×10^{-5} m^3 s^{-1}). The volume-based specific aeration rates used in this study (i.e., 3.8×10^{-4} to 2.3×10^{-3} m^3 m^{-3} d^{-1}) were smaller than the biogas production rates of 0.03 to 0.23 m^3 m^{-3} d^{-1} from treatment lagoons reported by Safley and Westerman (1988), but the surface-based specific aeration rates (i.e., 0.05 to 0.93 m^3 m^{-2} d^{-1}) were larger than the biogas production rates of 0.02 to 0.5 m^3 m^{-2} d^{-1} in the same report. Thus, our experimental conditions for bubbling were within the realm of actual field conditions.

At the onset of the experiments, appropriate amounts of concentrated NH_4OH were added to the pan water (distilled water) to yield initial ammonia concentrations in water ranging from 150 to 350 g m^{-3}. The clear PVC column water was spiked with a higher concentration of ammonia (about 4,500 g m^{-3}) to amplify the impact of bubbles on ammonia volatilization rates. The pan water and the PVC column water were well mixed, and the ammonia concentrations were uniform during the test periods. Hourly samples of 20 cm^3 pan water and daily samples of PVC column water were collected and immediately analyzed for NH_3 with a Corning gas-sensing ammonia combination electrode (Part No. 300740.0, Cole Palmer, Vernon Hills, Ill.). Temperatures and pH of the samples were measured with a multi-probe pH meter (556 MPS, YSI, Yellow Springs, Ohio). Wind speed and direction (5 min averages) and air temperature were measured at 10 m from a micrometeorological station near the pans, which is equipped with a cup anemometer (CS800-L Climatronics, Campbell Scientific, Logan, Utah) and a temperature sensor (Vaisala temperature probe, Campbell Scientific, Logan, Utah).

The ammonia concentration decreased with time, as ammonia was volatilized from water to air. If the container is modeled as an ideal batch reactor, the mass balance of ammonia in the container gives:

$$\frac{dC_{T,B}}{dt}V = -K_L A\left(FC_{T,B} - \frac{P_{N,B}}{K_H}\right) \quad (21)$$

Bulk air ammonia concentration ($P_{N,B}$) was undetectable and assumed zero at the experimental site. The average pH values of pan water and PVC column water ranged from 9.6 to 10.6 with less than 0.3 standard deviations for the duration of each experiments (i.e., about 7 hours for pan tests and 10 days for the column test). Assuming constant pH and T for the duration of experiments, equation 21 can be integrated with zero bulk air ammonia concentration to give:

$$C_{T,B}(t) = C_0 \cdot \exp\left(\frac{-FK_L t}{d}\right) \quad (22)$$

where

C_0 = initial total ammonia concentration (g m^{-3})

d = water depth (m).

As recommended by the ASCE Standard Method (ASCE, 1992) for oxygen transfer test, the two parameters C_0 and K_L were estimated simultaneously via non-linear regression analysis. GeoPad Prism (GraphPad Software, Inc., San Diego, Cal.) was used for the non-linear regression analysis. The difference between the reciprocals of the overall mass transfer coefficients determined from bubble-enhanced and non-bubble containers represents the negative bubble resistance as:

$$R_B = \frac{1}{K_{L,c}} - \frac{1}{K_{L,B}} \quad (23)$$

where

$K_{L,c}$ = overall mass transfer coefficient of non-bubble control container (m s^{-1})

$K_{L,B}$ = overall mass transfer coefficient of bubble-enhanced container (m s^{-1}).

Results and Discussion

Estimation of Bubble Resistance

Figure 4 shows the total ammonia concentration profile of the columns during test periods. The exponential decay pattern predicted by equation 22 generally fitted the data moderately well, as indicated by R^2 values ranging from 0.75 to 0.98 (table 2). At a specific aeration rate of 2.3 × 10^{-3} m^3 m^{-3} d^{-1}, the ammonia mass transfer coefficient of the bubble column was about 75% larger than that of the control column. For the pan water, the aeration increased K_L from 4% to 38% compared to that of non-aerated control pan, as shown in table 2 and figure 5. The bubble resistances (R_B) for each experimental run were estimated using equation 23 (table 2). The average value of R_B for the pan water varied from 8.5 × 10^3 to 1.9 × 10^5 s m^{-1} (average value of 6.3 × 10^4 s m^{-1}). The R_B for the column water (3.3 × 10^5 s m^{-1}) was larger than that for pan water.

The applicability of equation 17 was investigated by estimating the overall mass transfer coefficients of bubble-enhanced containers. The individual liquid-phase oxygen mass transfer coefficient at a specific aeration rate from equation 17 was converted to $k_{L,NH3}$ using equation 6 with n = 0.5. The individual gas-phase water vapor mass transfer at a 10 m wind speed from equation 7 was converted to $k_{G,NH3}$ using equation 6 with n = 0.67. The overall liquid-phase ammonia mass transfer coefficient was then estimated using

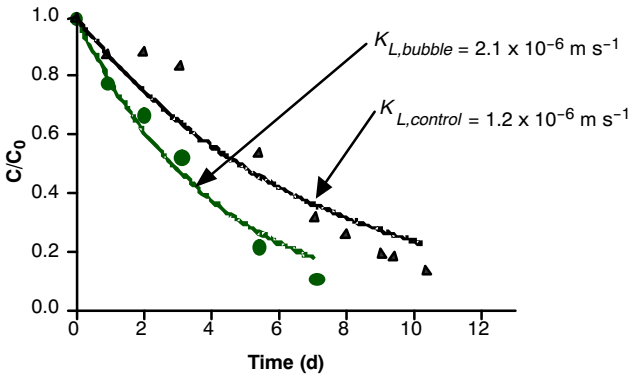

Figure 4. NH_3 profiles of the columns.

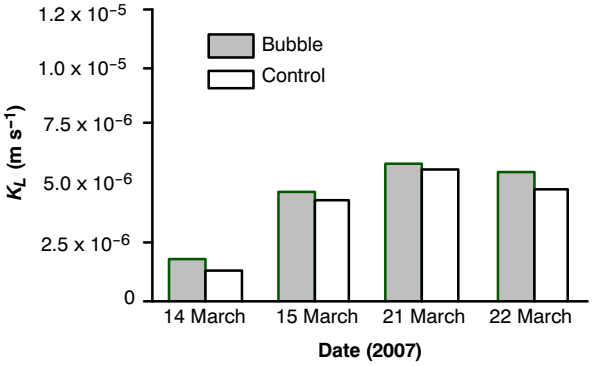

Figure 5. Comparison of K_L for ammonia volatilization from evaporation pans.

Table 2. NH_3 volatilization mass transfer coefficients from pan and column tests.

Date (2007)	Type	Aeration Q/V (m^3 m^{-3} d^{-1})	K_L (m s^{-1}) Experiments	R^2	K_L (m s^{-1}) Using eq. 17	R_B (s^{-1} m)
14 March	Pan	3.8 × 10^{-4}	1.8 × 10^{-6}	0.75	6.8 × 10^{-6}	1.9 × 10^5
		0	1.3 × 10^{-6}	0.78	N/A	
15 March	Pan	7.9 × 10^{-4}	4.7 × 10^{-6}	0.85	4.1 × 10^{-6}	2.4 × 10^4
		0	4.2 × 10^{-6}	0.89	N/A	
21 March	Pan	7.9 × 10^{-4}	5.9 × 10^{-6}	0.96	1.9 × 10^{-6}	8.5 × 10^3
		0	5.7 × 10^{-6}	0.93	N/A	
22 March	Pan	8.0 × 10^{-4}	5.5 × 10^{-6}	0.96	1.6 × 10^{-6}	2.6 × 10^4
		0	4.8 × 10^{-6}	0.96	N/A	
3-14 April	Column	2.3 × 10^{-3}	2.1 × 10^{-6}	0.98	5.0 × 10^{-6}	3.3 × 10^5
		0	1.2 × 10^{-6}	0.93	N/A	

Table 3. Characteristics of flushed swine manure liquid being discharged into the lagoons for the three lagoon treatment scenarios at Goshen Ridge Farm, Duplin County, North Carolina.[a]

Lagoon[b]	TSS (mg L^{-1})	VSS (mg L^{-1})	COD (mg L^{-1})	BOD (mg L^{-1})	TKN (mg L^{-1})	Organic N (mg L^{-1})	TAN (mg L^{-1})
Non-treated	9156 ±7129	7380 ±6885	14511 ±10826	2806 ±2581	1366 ±538	588 ±337	778 ±282
Partially treated	710 ±527	621 ±481	3043 ±2357	697 ±572	703 ±257	79 ±68	630 ±205
Treated	264 ±154	85 ±50	445 ±178	7 ±8	23 ±24	11 ±12	11 ±20

[a] Data are means ± standard deviation of duplicate weekly composite samples during one year. TSS = total suspended solids, VSS = volatile suspended solids, COD = chemical oxygen demand, BOD = five-day biochemical oxygen demand, TKN = total Kjeldahl N, TAN = total ammoniacal N, and Organic N = TKN - TAN.

[b] Non-treated = lagoon received raw flushed manure (traditional anaerobic lagoon); Partially treated = lagoon received the liquid from liquid-solid separation unit that treated the flushed raw manure; Treated = lagoon received depurated liquid manure after going through liquid-solid separation, biological N removal and P treatment.

equation 16 with $k_{L,NH3}$, $k_{G,NH3}$, K_H, and R_B. The values of K_L using equation 17 predicted several times lower or higher than observed values except for the data on 15 March 2007, as shown in table 2. Therefore, equation 17 should be used with caution in estimating bubble-enhanced mass transfer coefficients for ammonia volatilization from treatment lagoons.

Validation of the Model

Lagoon Scenarios

Our new process model for ammonia volatilization incorporating wind distribution and bubbling was validated using NH_3 emissions and water quality data from three swine lagoons at Goshen Ridge Farm near Mount Olive, Duplin County, North Carolina (Szogi et al., 2006; Szogi and Vanotti, 2006). The farm had three finishing units under identical animal production. Each unit had six barns with 4,360-head finishing pigs and an anaerobic lagoon for treatment and storage of manure. Manure was collected in barns using slatted floors and a pit-recharge system typical of many farms in North Carolina (Barker, 1996). Manure accumulated in the pits was flushed weekly by gravity, and raw manure from each production unit received a separate, different treatment.

In unit 1, flushed raw manure was stored and treated using typical anaerobic lagoon management (hereafter called non-treated lagoon) with a detention time of about 180 d; lagoon effluent was used to recharge the barn pits. In unit 2, a solid-liquid separation system partially treated raw manure flushed from the barns prior to lagoon storage. The raw manure was reacted with a flocculent polymer (polyacrylamide) and separated with a self-cleaning rotating screen (0.25 mm opening). Subsequently, a small filter press dewatered the manure solids. The separated liquid was stored in the lagoon (hereafter called partially treated lagoon) and later used to refill the barn pit recharge system. Separated solids generated in unit 2 were transported off-site and processed into value-added products (Szogi and Vanotti, 2006).

In unit 3, a full-scale wastewater treatment system treated all raw manure. The treatment system combined solid-liquid separation as in unit 2 with removal of nitrogen and phosphorus from the liquid phase. The system treated raw manure flushed from the barns in three steps (Vanotti et al., 2006). The first step flocculated solids from raw flushed manure using polyacrylamide. This step produced separated solids that were transported off-site and converted to organic plant fertilizer, soil amendments, or energy at a centralized facility. In the second step, N management to reduce ammonia emissions was accomplished by passing the liquid through a module where immobilized nitrifying bacteria transformed ammonia into nitrate, and denitrifying sludge further transformed nitrate into dinitrogen gas. Subsequent alkaline treatment of the wastewater in a P module precipitated calcium phosphate and killed pathogens. The treated water was recycled to refill the barn pit recharge system, and excess water was stored in the lagoon and later used for crop irrigation. As the treatment system recovered the manure solids and replaced the anaerobic lagoon liquid with cleaner water, it converted the anaerobic lagoon in unit 3 into a treated water pond (hereafter called treated lagoon).

For each of the three scenarios, flushed manure had large differences in water quality prior to lagoon input due to different pre-treatments (table 3). The non-treated lagoon received both a high organic and inorganic N (TAN) load (table 4). In the partially treated lagoon, the solid-liquid separation removed organic components of the raw flushed manure (VSS, BOD, and organic N), but it barely removed inorganic N because most inorganic N is in soluble form as TAN. With total pre-treatment of flushed manure, both organic and TAN components were removed, producing a substantially cleaner effluent for the treated lagoon. It is important to notice that recovery of manure solids prior to lagoon input in both the partially treated and treated lagoons greatly reduced the organic substrate (VSS, BOD, and organic N) for anaerobic microbial processes that produce biogas; consequently, gas bubbling activity was dramatically reduced.

During 2004, ammonia emissions were measured in all three lagoons using passive flux samplers following the method of Sommer et al. (1996). Nine simultaneous data collection periods lasting 23 h each were scheduled from February to November 2004 for the three lagoons. Further details on NH_3 emission measurements using the passive flux method are described by Szogi et al. (2006). Even though animal production management remained the same in all three production units, substantially different manure treatment in each unit significantly affected the total annual ammonia emissions. The non-treated anaerobic lagoon had the highest annual measured ammonia emissions (13,633 kg ha^{-1} $year^{-1}$), while the partially treated anaerobic lagoon and the treated lagoon had about 30% (3,699 kg ha^{-1} $year^{-1}$) and

Table 4. Organic and total ammoniacal loads relative to non-treated lagoon in the three lagoon treatment scenarios at Goshen Ridge Farm, Duplin County, North Carolina.

Lagoon	Organic Load	Total Ammoniacal N Load
Non-treated	High	High
Partially treated	Low	High
Treated	Low	Low

Table 5. Observed ammonia emission data from the three lagoons of Goshen Ridge Farm in 2004.[a]

Lagoon	Season	Sample Size (n)	Flux (kg-N ha^{-1} d^{-1})	T_{water} (˚C)	T_{air} (˚C)	$C_{T,N}$ (g-N m^{-3})	pH
Non-treated	Winter	2	3.5 ±1.4	9.6 ±4.3	7.0 ±2.0	376.7 ±65.9	7.9 ±0.2
	Spring	3	42.0 ±31.9	22.2 ±7.5	17.2 ±9.8	463.8 ±50.2	7.9 ±0.1
	Summer	2	71.0 ±3.5	28.9 ±1.8	25.9 ±0.1	316.0 ±29.1	8.1 ±0.1
	Fall	2	33.6 ±27.6	20.3 ±6.9	12.7 ±11.2	268.3 ±39.2	8.2 ±0.1
Partially treated	Winter	2	3.5 ±1.4	9.5 ±4.3	4.3 ±0.2	462.0 ±56.6	7.9 ±0.2
	Spring	3	8.3 ±2.5	20.0 ±6.5	17.0 ±9.7	429.8 ±124.9	7.9 ±0.3
	Summer	2	25.9 ±2.3	27.4 ±1.8	26.0 ±0.0	267.7 ±28.9	8.3 ±0.1
	Fall	2	8.1 ±8.1	19.5 ±6.6	12.8 ±11.5	178.7 ±22.9	8.2 ±0.2
Treated	Winter	2	2.1 ±1.6	9.6 ±4.3	7.5 ±1.4	44.0 ±35.5	8.0 ±0.2
	Spring	2	5.4 ±1.8	22.3 ±7.2	17.2 ±9.8	48.8 ±35.1	7.9 ±0.1
	Summer	2	11.8 ±1.1	28.7 ±0.1	25.6 ±0.0	50.3 ±28.6	8.1 ±0.2
	Fall	2	1.2 ±0.1	19.6 ±7.7	13.3 ±11.1	1.3 ±2.3	8.3 ±0.6

[a] Data from Szogi et al., 2006; Szogi and Vanotti, 2007.

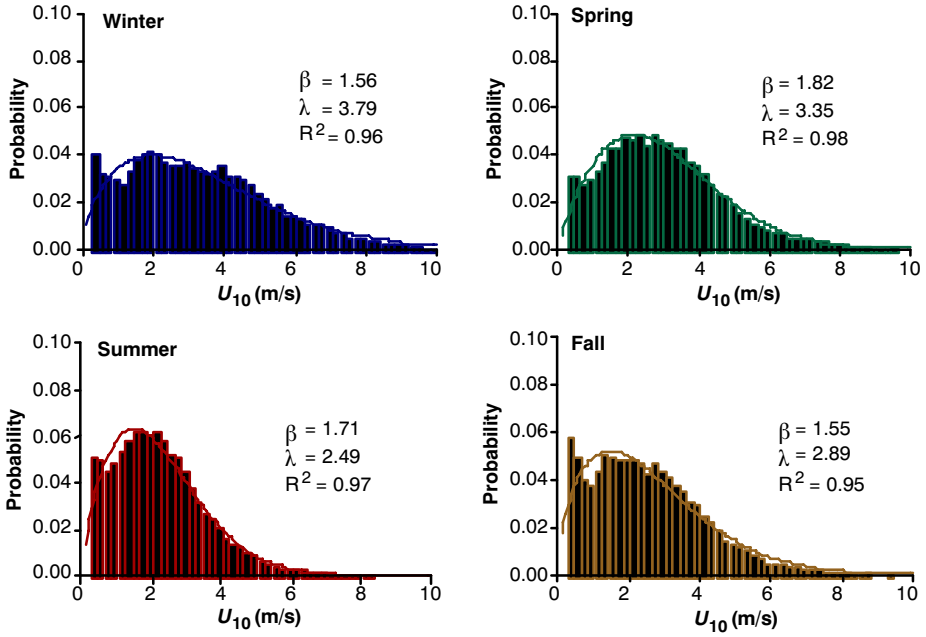

Figure 6. Weibull wind speed distributions of the field site during study periods.

Table 6. Ammonia emission simulation results.

Lagoon	Season	Observed Flux[a] J_O (kg N ha^{-1} d^{-1})	Mean K_L (m s^{-1})	Simulated Flux J_S (kg N ha^{-1} d^{-1})	Relative Error, $(J_S - J_O)/J_O$ (%)	Bubble Resistance Used for Simulation (s m^{-1})
Non-treated	Winter	3.5 ±1.4	1.8×10^{-6}	4.1	18	0
	Spring	42.0 ±31.9	5.6×10^{-6}	40.6	-3	8.23×10^{4}
	Summer	71.0 ±3.5	5.5×10^{-6}	64.2	-10	8.23×10^{4}
	Fall	33.6 ±27.6	4.9×10^{-6}	35.1	5	8.23×10^{4}
Partially treated	Winter	3.5 ±1.4	1.8×10^{-6}	4.9	37	0
	Spring	8.3 ±2.5	2.6×10^{-6}	15.3	85	0
	Summer	25.9 ±2.3	2.5×10^{-6}	31.9	23	0
	Fall	8.1 ±8.1	2.0×10^{-6}	9.0	11	0
Treated	Winter	2.1 ±1.6	1.8×10^{-6}	1.1	-49	0
	Spring	5.4 ±1.8	2.8×10^{-6}	4.3	-21	0
	Summer	11.8 ±1.1	2.6×10^{-6}	6.2	-47	0
	Fall	2.4 ± 0.1	2.0×10^{-6}	0.2	-86	0

[a] Data from Szogi et al., 2006; Szogi and Vanotti, 2007.

about 10% (1,311 kg ha^{-1} year^{-1}) of the annual ammonia emissions with respect to the non-treated lagoon, respectively (Szogi et al., 2006; Szogi and Vanotti, 2007). The seasonal ammonia fluxes from these lagoons along with relevant water quality and air and water temperatures are summarized in table 5.

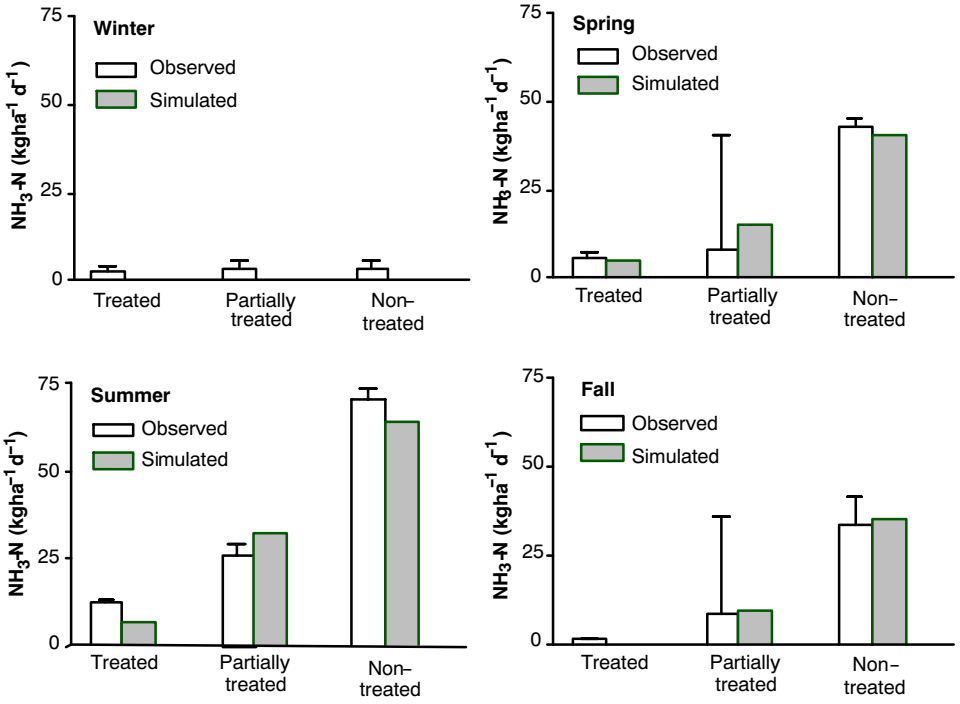

Figure 7. Comparison of simulated and observed ammonia volatilization rates from the field site (observed values based on data from Szogi et al., 2006; Szogi and Vanotti, 2007).

Simulation Results

The two-parameter Weibull distribution adequately characterized the 5 min average wind speed distributions of the field site during the study periods. The wind speed data were collected from 1 January to 1 December 2004 using a wind sensor (R.M. Young Co., Traverse City, Mich.) mounted at 2.5 m height. The 10 m wind speed was then estimated using the logarithmic profile with a surface roughness of 0.03 m (Ro and Hunt, 2007). As shown in figure 6, the Weibull probability density function fit the observed wind speed frequency distributions for all seasons with R^2 ranging from 0.95 to 0.98. Although the wind speeds larger than the lowest recordable threshold speed of 0.2 m s^{-1} were fitted nicely to the Weibull probability density function, 10% to 16% of all wind speed measurements were below the threshold speed and, thus, were not part of the distributions. If we treat this portion of the data (i.e., wind speed $\leq$ 0.2 m s^{-1}) as zero wind speed, then equations 7 and 8 are no longer valid to simulate the mass transfer coefficients. For the near-zero wind portion of the data, we assumed constant values of the oxygen liquid-phase mass transfer coefficient of 4.0×10^{-6} m s^{-1} and the water vapor gas-phase mass transfer coefficient of 4.8×10^{-5} m s^{-1}, as suggested by other researchers (Gualtieri, 2006; Schwarzenbach et al., 1993). The overall mean mass transfer coefficients were then determined from weighted average of the near-zero wind mass transfer coefficients and the mass transfer coefficient based on the Weibull wind distributions (for $U_{10} > 0.2$ m s^{-1}) estimated using equations 4, 5, 6, 7, 8, and 16.

Because significant bubbling was observed only in the non-treated lagoon during warm seasons, the best values of bubble resistance were estimated from fitting the observed fluxes of the non-treated lagoon during spring, summer, and fall seasons. The fitted bubble resistance for the non-treated lagoon varied little from 8.22×10^4 to 8.24×10^4 s m^{-1} for the three warm seasons, with an average value of $8.23 \times 10^4 \pm 60$ s m^{-1}, about 31% higher than that for the pan water, but 75% lower than that for the column water.

This average bubble resistance was then applied to estimate the overall mass transfer coefficient (eq. 16) for the non-treated lagoon. Once the mean values of overall mass transfer coefficients for each season were determined, the average ammonia volatilization rates were then simulated according to equation 2. Table 6 and figure 7 show the observed and simulated ammonia fluxes from the three lagoons. In order to evaluate the effect of bubbling on the ammonia volatilization of the non-treated lagoon, the model was also simulated with zero bubble resistance. As shown in figure 8, the model would significantly underestimate ammonia volatilization rates during warm seasons if the bubbling-enhanced mass transfer had not been considered.

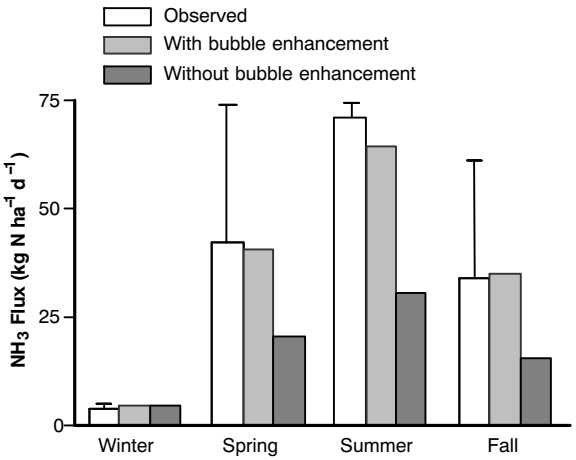

Figure 8. Comparison of ammonia fluxes from the non-treated lagoon, observed and simulated with and without bubble enhancement (observed values based on data from Szogi et al., 2006; Szogi and Vanotti, 2007).

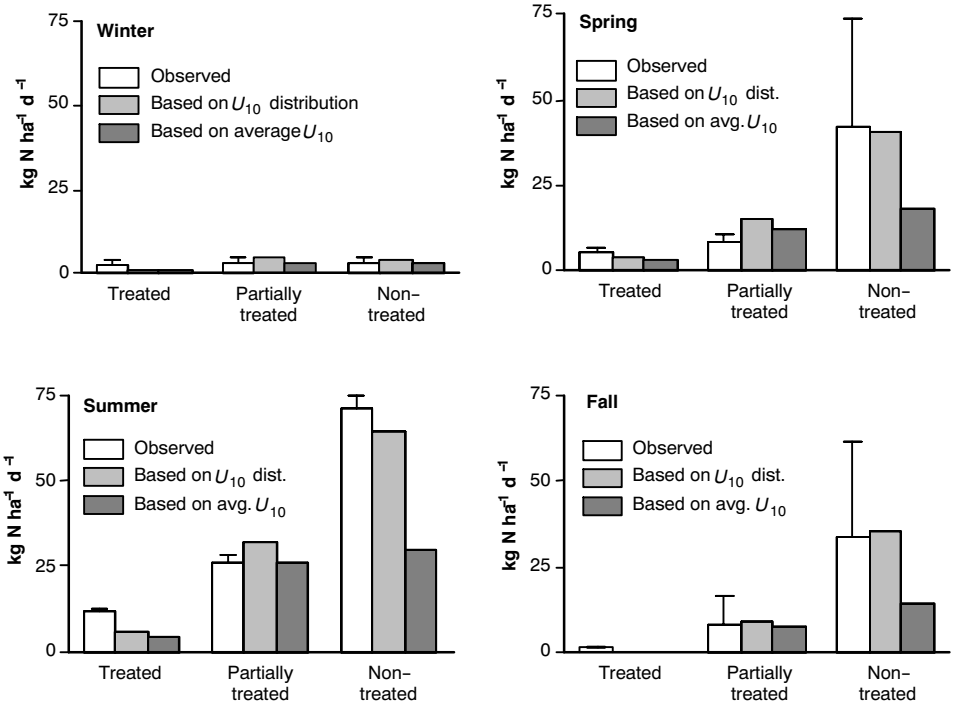

Figure 9. Comparison of simulated ammonia fluxes using arithmetic U_{10} averages and U_{10} distributions (observed values based on data from Szogi et al., 2006; Szogi and Vanotti, 2007).

We also tested the impact of using simple arithmetic average U_{10} for each season in simulating ammonia fluxes instead of U_{10} distributions. Figure 9 shows that ammonia fluxes based on average U_{10} simulated as well as U_{10} distributions for the treated and partially treated lagoons. However, the ammonia fluxes from the non-treated lagoon simulated by the average U_{10} significantly underestimated the actual ammonia emission for warm seasons, similar to the bubbling vs. non-bubbling effects in figure 8. Figure 10 plots the entire observed ammonia emission data from the three lagoons of Goshen Ridge Farm in 2004 vs. simulated fluxes obtained from three different procedures. The simulated fluxes using the U_{10} distributions along with bubble enhancement for the non-treated lagoon during warm seasons closely matched the observed fluxes (y = 1.04x, with R^2 = 0.76). The simulations using average U_{10} with bubble enhancement or U_{10} distributions without bubble enhancement produced fluxes 42% and 44%, respectively, below observed fluxes.

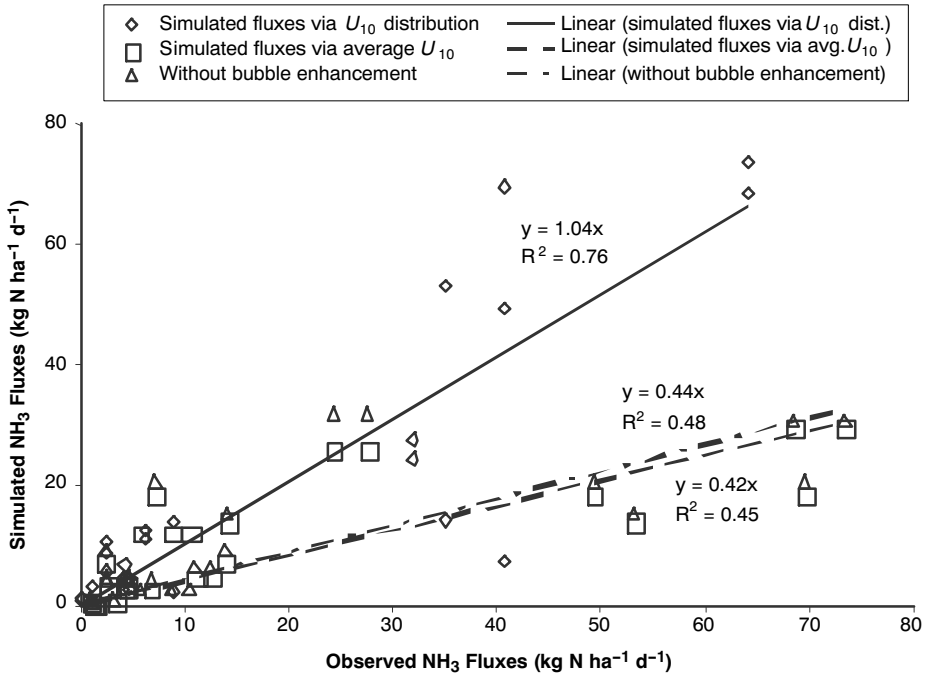

Figure 10. Comparison of simulated ammonia fluxes with U_{10} distribution, average U_{10}, and without bubble enhancement.

Conclusions

This article developed a new process-based ammonia volatilization model integrating the ammonia chemistry in lagoon liquid and the complex air-water interfacial mass transfer phenomena, including the bubbling effects of the lagoon liquid by anaerobic microbial activity. Instead of using an average wind speed, this model simulated mean overall mass transfer coefficients from integrating the mass transfer coefficient correlations over the entire wind field of the site. The model simulated reasonably well the ammonia emissions measured from three lagoons with distinct manure management and water quality characteristics. The average bubble resistance for the non-treated lagoon during warm seasons was 8.23×10^4 s m^{-1}. Ammonia emission prediction would be significantly improved when bubbling-enhanced mass transport is accounted for during warm seasons, as demonstrated by the model and evidenced by the observed fluxes.

Acknowledgements

This research was part of USDA-ARS National Program 206: Manure and Byproduct Utilization; ARS Project 6657-13630-003-00D "Innovative Animal Manure Treatment Technologies for Enhanced Environmental Quality." The writers are indebted to Mr. M. Johnson for the collection, organization, and processing of a large volume of meteorological data.

References

Anderson, G. A., R. J. Smith, D. S. Bundy, and E. G. Hammond. 1987. Model to predict gaseous contaminants in swine confinement buildings. *J. Agric. Eng. Res.* 37(3-4): 235-253.

Arogo, J., R. H. Zhang, G. L. Riskowski, L. L. Christianson, and D. L. Day. 1999. Mass transfer coefficient of ammonia in liquid swine manure and aqueous solutions. *J. Agric. Eng. Res.* 73(1): 77-86.

Arogo, J., P. W. Westerman, and A. J. Heber. 2003a. A review of ammonia emissions from confined swine feeding operations. *Trans. ASAE* 36(3): 805-817.

Arogo, J., P. W. Westerman, and Z. S. Liang. 2003b. Comparing ammonium ion dissociation constant in swine anaerobic lagoon liquid and deionized water. *Trans. ASAE* 46(5): 1415-1419.

ASCE. 1992. *Standard ASCE Measurement of Oxygen Transfer in Clean Water.* New York, N.Y.: ASCE.

Bajwa, K. S., V. P. Aneja, and S. P. Arya. 2006. Measurement and estimation of ammonia emissions from lagoon-atmosphere interface using a coupled mass transfer and chemical reactions model, and equilibrium model. *Atmos. Environ.* 40(suppl. 2): 275-286.

Barker, J. C. 1996. Lagoon design and management for livestock waste treatment and storage. Pub. No. EBAE 103-83. Raleigh, N.C.: North Carolina Cooperative Extension Service.

Blunden, J., and V. P. Aneja. 2007. Characterizing ammonia and hydrogen sulfide emissions from a swine waste treatment lagoon in North Carolina. 2007. *Atmos. Environ.* (in press).

Crowe, C. T., D. F. Elger, and J. A. Roberson. 2001. Appendix. In *Engineering Fluid Mechanics*, A6-A14. 7th ed. New York, N.Y.: John Wiley and Sons.

Cussler, E. L. 1984. *Diffusion Mass Transfer in Fluid Systems.* New York, N.Y.: Cambridge University Press.

De Visscher, A., L. A. Harper, P. W. Westerman, Z. Liang, J. Arogo, R. R. Sharpe, and O. Van Cleemput. 2002. Ammonia emission from anaerobic swine lagoons: Model development. *J. Applied Meteorology* 41(4): 426-433.

Frank, M. J. W., J. A. M. Kuipers, and W. P. M. van Swaaij. 1996. Diffusion coefficients and viscosities of CO_2 + H_2O, CO_2 + CH_3OH, NH_3 + H_2O, and NH_3 + CH_3OH liquid mixtures. *J. Chem. Eng. Data* 41(2): 297-302.

Fuller, E. N., P. D. Schettler, and J. C. Giddings. 1966. A new method for prediction of binary gas-phase diffusion coefficients. *Ind. Eng. Chem.* 58(5): 18-27.

Gottschalk, C., J. A. Libra, and A. Saupe. 2000. *Ozonation of Water and Wastewater.* New York, N.Y.: Wiley-VCH.

Gualtieri, C. 2006. Verification of wind-driven volatilization models. *Environ. Fluid Mech.* 6(1): 1-24.

Hamilton, D. W., I. N. Kourtchev, P. M. Ndegwa, H. J. Cumba, and F. Gioelli. 2006. Methane and carbon dioxide emissions from simulated anaerobic swine manure treatment lagoons under summer conditions. *Trans. ASABE* 49(1): 157-165.

Harper, L. A., R. R. Sharpe, and T. B. Parkin. 2000. Gaseous nitrogen emissions from anaerobic swine lagoons: Ammonia, nitrous oxide, and dinitrogen gas. *J. Environ. Qual.* 29(4): 1356-1365.

Harper, L. A., R. R. Sharpe, T. B. Parkin, A. De Visscher, O. van Cleemput, and F. M. Byers. 2004. Nitrogen cycling through swine production systems: Ammonia, dinitrogen, and nitrous emissions. *J. Environ. Qual.* 33(4): 1189-1201.

Hsieh, C. C. 1991. Estimating volatilization rates and gas/liquid mass transfer coefficients in aeration systems. PhD diss. Los Angeles, Cal.: University of California.

Hsieh, C. C., K. S. Ro, and M. K. Stenstrom. 1993. Estimating emissions of 20 VOCs: I. Surface aeration. *J. Environ. Eng.* 119(6): 1077-1098.

Lewis, W. K., and W. G. Whitman. 1924. Principles of gas absorption. *Ind. and Eng. Chem.* 16(12): 1215-1220.

Liang, Z. S., P. W. Westerman, and J. Arogo. 2002. Modeling ammonia emission from swine anaerobic lagoons. *Trans. ASAE* 45(3): 787-798.

Liss, P. S. 1973. Processes of gas exchange across an air-water interface. *Deep-Sea Res.* 20: 221-238.

Macintyre, S., R. Wahhninkhof, and J. P. Chanton. 1995. Tracer gas exchange across the air-water interface in fresh waters and coastal marine environments. In *Biogenic Trace Gases: Measuring Emission from Soil and Water*, 52-97. P. A. Matson and R. C. Harris, eds. Malden, Mass.: Blackwell.

Mackay, D., and A. T. K. Yeun. 1983. Mass transfer coefficient correlations for volatilization of organic solutes from water. *Environ. Sci. Tech.* 17(4): 211-217.

Monteny, G.-J. 2000. Modeling of ammonia emissions from dairy cow houses. PhD diss. Wageningen, The Netherlands, Wageningen University.

Ni, J. 1999. Mechanistic models of ammonia release from liquid manure: A review. *J. Agric. Eng. Res.* 72(1): 1-17.

Ro, K. S., and P. G. Hunt. 2006. A new unified equation for wind-driven surficial oxygen transfer into stationary water bodies. *Trans. ASABE* 49(5): 1615-1622.

Ro, K. S., and P. G. Hunt. 2007. The effect of averaging time on characteristic wind speed distributions and the accuracy of the logarithmic wind profile. *J. Environ. Eng.* 133(3): 313-318.

Ro, K. S., P. G. Hunt, and M. E. Poach. 2007. Wind-driven surficial oxygen transfer. *Critical Reviews Environ. Sci. Tech.* 37(6): 539-563.

Safley, Jr., L. M., and P. W. Westerman. 1988. Biogas production from anaerobic lagoons. *Biol. Wastes* 23(3): 181-193.

Schwarzenbach, P. R., P. M. Gschwend, and D. M. Imboden. 1993. Chapter 10. In *Environmental Organic Chemistry*, 215-241. New York, N.Y.: Wiley-Interscience.

Sharpe, R. R., and L. A. Harper. 1999. Methane emissions from an anaerobic swine lagoon. *Atmos. Environ.* 33(22): 3627-3633.

Sommer, S. G., E. Sibbesen, T. Nielsen, J. K. Schjorring, and J. E. Olesen. 1996. A passive flux sampler for measuring manure storage facilities. *J. Environ. Qual.* 25(2): 241-247.

Szogi, A. A., and M. B. Vanotti. 2006. Reduction of ammonia emissions from swine lagoons using alternative wastewater treatment technologies. In *Workshop on Agricultural Air Quality: State of the Science*, 1155-1160. Washington, D.C.: Ecological Society of America.

Szogi, A. A., and M. B. Vanotti. 2007. Abatement of ammonia emissions from swine lagoons using polymer-enhanced solid-liquid separation. *Applied Eng. in Agric.* 23(6): 837-845.

Szogi, A. A., M. B. Vanotti, and A. E. Stansbery. 2006. Reduction of ammonia emissions from treated anaerobic swine lagoons. *Trans. ASABE* 49(1): 217-225.

Troen, I., and E. L. Peterson. 1989. *European Wind Atlas*. Brussels, Belgium: Commission of the European Communities Directorate-General for Science, Research and Development; and Roskilde, Denmark: Riso National Laboratory.

Vanotti, M. B., A. A. Szogi, P. G. Hunt, P. D. Millner, and F. J. Humenik. 2006. Development of environmentally superior treatment systems to replace anaerobic swine lagoons in the USA. *Bioresource Tech.* 98(17): 3184-3194.

Upstill-Goddard, R. C., A. J. Watson, P. S. Liss, and M. I. Liddicoat. 1990. Gas transfer velocities in lakes measured with SF_6. *Tellus B* 42(4): 364-377.

Wanninkhof, R. 1992. Relationship between wind speed and gas exchange over the ocean. *J. Geophys. Res.* 97(C5): 7373-7382.

USEPA. 2001. Environmental assessment of proposed revisions to the national pollutant discharge elimination system regulation and the effluent guidelines for concentrated animal feeding operations. EPA-821-B-01-001, Chapters 2-3. Washington, D.C.: U.S. EPA.

Zhang, R. H. 1992. Degradation of swine manure and a computer model for predicting the desorption rate of ammonia from an under-floor pit. PhD diss. Urbana, Ill.: University of Illinois.